JOURNAL OF SOLID STATE CHEMISTRY **140,** 83–90 (1998)
ARTICLE NO. SC987863

Selective Deposition of UCl_4 and $(KCl)_x(UCl_4)_y$ inside Carbon Nanotubes Using Eutectic and Noneutectic Mixtures of UCl_4 with KCl

J. Sloan,*,† J. Cook,* A. Chu,* M. Zwiefka-Sibley,* M. L. H. Green,*,[1] and J. L. Hutchison†

*Inorganic Chemistry Laboratory, University of Oxford, South Parks Road, Oxford OX1 3QR, United Kingdom; and †Department of Materials, University of Oxford, Parks Road, Oxford, OX1 3PH, United Kingdom

Received August 28, 1996; in revised form April 21, 1998; accepted April 22, 1998

UCl_4 and compositions of the form $(KCl)_x(UCl_4)_y$ have been selectively deposited inside multiple-walled carbon nanotubes (MWTs) via capillary action using both eutectic and noneutectic mixtures of UCl_4 with KCl. The deposition conditions were determined from the pseudobinary KCl–UCl_4 phase diagram, which contains two eutectic melting compositions at 50 mol% KCl : 50 mol% UCl_4 and 73.2 mol% KCl : 26.8 mol% UCl_4, and also from surface tension/composition data reported in the literature. The encapsulated products were investigated by HRTEM and EDX incorporating both nanometer and sub-nanometer scale electron probes. Following preliminary characterization, the selectively encapsulated UCl_4 was allowed to oxidize in air for 14 days, but only a relatively small amount (ca. 2%) of a crystalline oxidized product of the form $U(Cl, O)_x$ was observed inside the MWTs. Some MWTs selectively filled with UCl_4 showed evidence of spiraling (helical) crystal growth.

INTRODUCTION

The capillaries of multiple-walled carbon nanotubes (MWTs) have proven to be an interesting medium for investigating the crystallization behavior of solid phase materials (1–6). These studies have been prompted by a desire to synthesize hybrid materials with novel physical properties on the nanometric scale (7). However, the small size of the MWT internal diameters (2–10 nm) occurs at the limits to which crystallization can be observed for many phases (1, 4, 6). Also, the mode of insertion dictates the nature and morphology of the obtained filling. For example, where deposition is induced via solution–deposition (2), small discrete encapsulates are obtained whereas when the filling is obtained via capillary filling, continuously filled MWTs are obtained (1, 4). For the synthesis of MWT composites with uniform physical properties, the most desirable strategy will be the latter although this method is only available to materials with sufficiently low surface tensions and melting points to fill MWTs without damaging them. Studies on the capillarity of MWTs indicate that the maximum threshold surface tension for the filling is in the range 100–200 mN/m (4). For example, only the oxides PbO, Bi_2O_3, V_2O_5, MoO_3, and B_2O_3 can successfully fill MWTs by the molten media method (4, 7).

Another possibility for obtaining filling by the capillary method is to use low-melting mixtures of phases in a binary or higher eutectic system that contains at least one melting temperature such that the resulting composition: (i) has an overall surface tension lower than the threshold value of 100–200 mN/m; (ii) has a sufficiently low melting temperature (< 1100 K) such that the carbon MWTs are not damaged thermally by the melt; and (iii) does not attack the MWTs chemically. We therefore describe here a study of molten media filling of MWTs achieved using various eutectic and noneutectic mixtures of KCl with UCl_4 and demonstrate how the phase relations within the system can be exploited to selectively fill MWTs with UCl_4 and other components within the KCl–UCl_4 system. We also describe the oxidation behavior of UCl_4 selectively deposited inside MWTs.

A study of the pseudobinary phase diagram of KCl–UCl_4 (Fig. 1), reconstructed here from the pseudoternary UCl_4–KCl–$ThCl_4$ phase diagram (8), shows that this system contains two eutectics at 50 mol% KCl : 50 mol% UCl_4 and 73.2 mol% KCl : 26.8 mol% UCl_4, respectively, and a third stable composition at 66.7 mol% KCl : 33.3 mol% UCl_4 (nominally K_2UCl_6). With respect to the thermodynamic and transport properties of the KCl–UCl_4 system, Janz *et al.* have established surface tension–temperature relationships for various compositions within the KCl–UCl_4 system (9). These can collectively be defined in terms of Eq. [1]:

$$s = a - bT, \qquad [1]$$

[1] To whom correspondence should be addressed.

0022-4596/98 $25.00

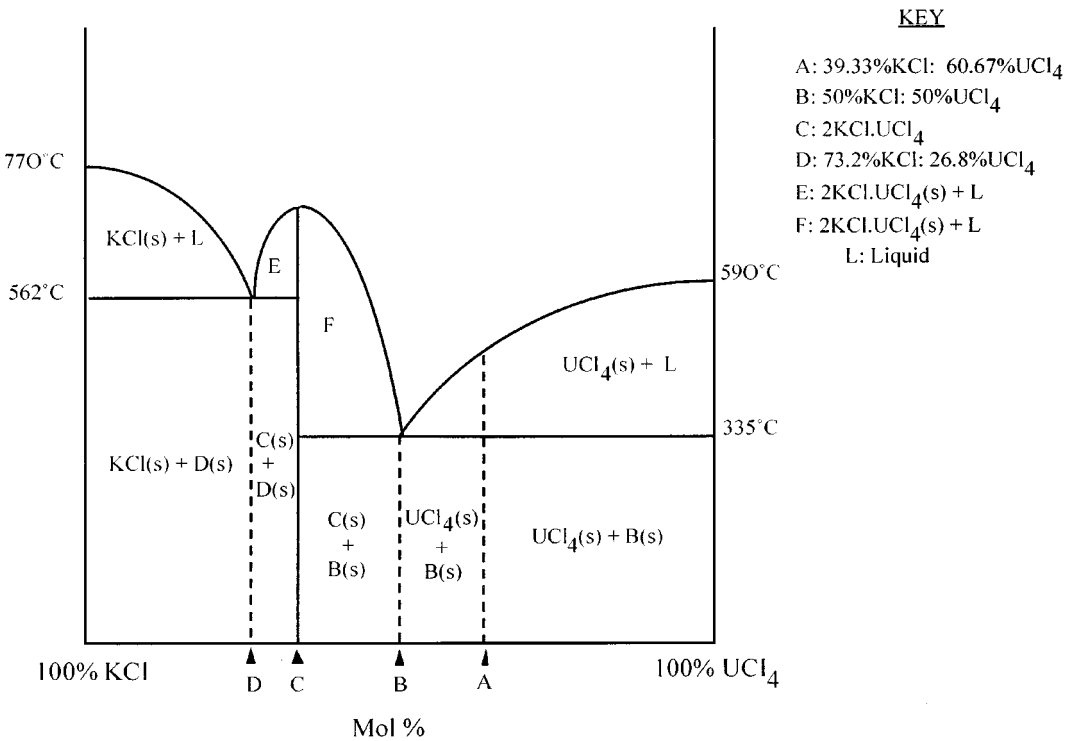

FIG. 1. Pseudobinary $KCl–UCl_4$ phase diagram showing compositions used to fill MWTs.

where s is the surface tension in mN/m, T is the temperature in K, and a and b are coefficients determined for a range of specific compositions and temperature ranges listed in Table 1a. For example, the surface tension of a noneutectic 39.33 mol% KCl : 60.67 mol% UCl_4 mixture (marked as composition A on Fig. 1) is 46.74 mN/m at 900 K, which is well below the threshold value for which solid filling of MWTs with molten media is predicted. This temperature is also too low to cause significant thermal damage to the MWTs. By contrast, the surface tension of pure UCl_4 at 900 K is 371.45 mN/m which is above the threshold value for which filling of MWTs is predicted via capillarity.

TABLE 1a
Compositions, *a* and *b* Coefficients, and Temperature Ranges for the $KCl–UCl_4$ Surface Temperature Relation, Eq. [1] (9)

$KCl–UCl_4$ (mol%)	*a*	*b*	Temperature range (K)
0–100	204.95	0.185	880–960
39.33–60.67	102.83	0.0621	890–980
56.04–43.96	93.04	0.04808	880–990
64.31–35.69	59.73	0.00865	930–1010
73.68–26.32	77.59	0.01349	870–1050
96.00–4.00	136.65	0.06732	1020–1150
97.33–2.67	164.82	0.08871	1050–1090
100–0	182.51	0.0782	1080–1170

EXPERIMENTAL

The MWTs used in this study were prepared by the modified standard are discharge technique described previously (10). The MWTs were selectively opened at their tips by refluxing in concentrated HNO_3 for 24 h and were subsequently decarboxylated by heating in air, according to established procedures (2, 3). For the various filling experiments, mixtures of KCl (Alfa, Specpure grade) and UCl_4

TABLE 1b
Compositions Used to Fill MWTs (See Also Fig. 1)

Compositions (see Fig. 1)	$KCl : UCl_4$ (mol%)	Liquidus temperature (K)	Calculated ST (mN/m)
UCl_4	0 : 100	863	371.45 at 900 K
A	39.33 : 60.67	742	46.74 at 900 K
B	50 : 50 (1 : 1)	608	120[a] at 750 K
C	66.7 : 33.3 (2 : 1)	~ 893	68[b] at 950 K
D	73.2 : 26.8	835	90[c] at 980 K
KCl	100 : 0	1043	270 at 1120 K

[a] Estimated from 56.04% KCl : 43.96% UCl_4 composition; probably lower at eutectic composition.

[b] Estimated from 64.31% KCl : 35.69% UCl_4 composition; may be higher due to formation of $2KCl \cdot UCl_4$ (K_2UCl_6).

[c] Estimated from 73.68% KCl : 26.32% UCl_4 composition.

(Strem, 97%) specified in Table 1b were intimately mixed in a 1:1 mass ratio with the opened, decarboxylated MWTs under drybox conditions and were then placed inside silica quartz ampules that were sealed under vacuum. Each mixture was then placed in a tube furnace preheated to ca. 150 K higher than the respective liquidus of the particular mixture and held at that temperature for 30 min, after which the ampules were allowed to furnace cool to room temperature. Small portions of each product were then removed for characterization. A portion of the product obtained using composition A (Table 1b) was subsequently allowed to oxidize in air for 14 days and was then characterized.

For subsequent high-resolution transmission electron microscopy (HRTEM) studies, the specimens were dispersed in chloroform in an ultrasonic bath for a period of 5 min and then placed dropwise onto lacey carbon-coated copper grids (Agar 200 mesh). Each specimen was initially characterized in a high-resolution JEM-4000EX microscope operated at 400 kV and then a JEM-2010 microscope operated at 200 kV. The JEM-2010 was equipped with a LINK Pentafet energy dispersive X-ray (EDX) analysis system with a 3 nm minimum probe size. The EDX spectra were analyzed with the LINK ISIS system. The oxidized specimen was characterized in a field emission gun (FEGTEM) JEM-2010F microscope operated at 200 kV equipped with a NORAN Voyager EDX system with a 0.7 nm minimum probe size.

RESULTS AND DISCUSSION

Selective Deposition of UCl_4 and $(KCl)_x(UCl_4)_y$ in MWTs

The results obtained for each of the compositions specified in Fig. 1 (see also Table 1b) are summarized in Table 2a. For the MWT filling experiments attempted with either of the pure components KCl and UCl_4 at the temperatures of 900 and 1120 K, respectively, no significant filling was observed via HRTEM. These results are consistent with both of the calculated surface tensions (270 and 371.45 mN/m, respectively) being too high relative to the maximum threshold surface tension (200 mN/m) for filling to occur. In the case of UCl_4, a coarse polycrystalline product was observed on the exterior of the opened MWTs, whereas in the case of KCl, a low-contrast, beam-sensitive crystalline product was observed external to the MWTs only.

TABLE 2a
Fillings Obtained with Compositions Specified in Table 1b (See Fig. 1)

Compositions	$KCl:UCl_4$ (mol%)	Filling temperature	Encapsulated product
UCl_4	0:100	900 K	None observed
A	39.33:60.67	900 K	Polycrystalline UCl_4
B	50:50 (1:1)	750 K	$KCl:UCl_4$ (1:1)
C	66.7:33.3 (2:1)	950 K	None observed
D	73.2:26.8	980 K	$KCl:UCl_4$ (~3:1)
KCl	100:0	1120 K	None observed

TABLE 2b
Measured and Corresponding Literature *d* Spacings and Corresponding Literature Values of Lattice Planes Observed in Encapsulated UCl_4 Crystallites

		d-spacing (Å)	
Crystallite no.	UCl_4 *hkl* plane	Measured	Literature (11)
I[a]	211	3.28	3.30
II[a]	211	3.29	3.30
III[b]	202	2.75	2.77
IV[b]	200	4.09	4.12
V[b]	202	2.75	2.77
V[b]	$20\bar{2}$	2.76	2.77
VI[c]	202	2.8	2.77
VII[c]	202	2.75	2.77
VIII[c]	202	2.76	2.77
IX[c]	202	2.76	2.77

[a] Fig. 1a.
[b] Fig. 1b.
[c] Fig. 7b.

The filling attempted with composition A produced selective filling of ca. 70% of all of the opened MWTs with UCl_4 only. HRTEM micrographs showed that UCl_4 was present as a polycrystalline material both on the inside and outside of MWTs, as shown in Fig. 2a, although EDX analyses indicated that the encapsulated product contained U and Cl only, while the external material contained U, Cl, and K. The MWT encapsulated crystallites (denoted **I** in Fig. 2a) were generally enlarged and somewhat elongated compared to the smaller spheroidal crystallites (denoted **II** in Fig. 2a) present in the polycrystalline material on the exterior of the MWTs. The *d*-spacings of the encapsulated crystallites, measured to within ± 0.05 Å relative to the (0001) fringes of the MWT walls (3.41 Å), could all be correlated with specific *hkl* planes of tetragonal UCl_4 (11). The lattice fringes of all of the crystallites denoted **I** in Fig. 2a correspond to (211) planes of tetragonal UCl_4. Note that these crystals exhibit varying orientations (denoted **I**, **I**′, **I**″, and **I**‴ in Fig. 2a relative to the MWT axis in Fig. 2a. The *d*-spacings of the crystallites denoted **II** in Fig. 2a also apparently conform to the same plane, suggesting that the UCl_4 in the material exterior to the MWTs is phase separated.

While the example in Fig. 2a shows an MWT capillary with discontinuous UCl_4 filling, more commonly the filling was continuous, as shown by the example in Fig. 3a, in accordance with the type of continuous and oriented filling reported for V_2O_5 (4) and MoO_3 (7). However, in the case of

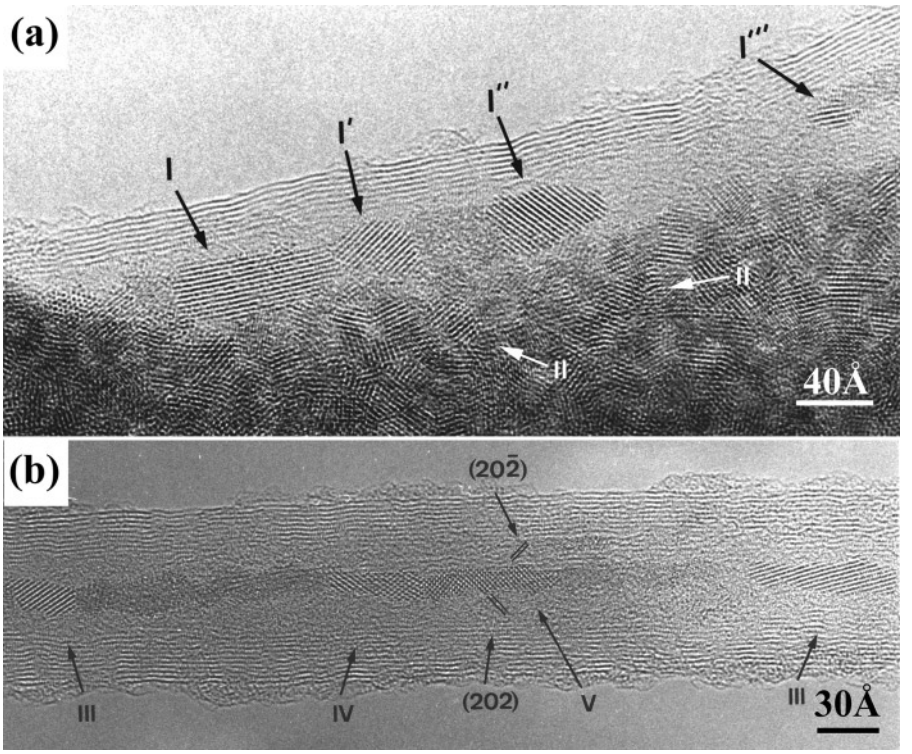

FIG. 2. (a) Micrograph showing bulk polycrystalline UCl_4/KCl material. A partially filled MWT can be seen on the surface of the material. (b) Micrograph showing continuous polycrystalline UCl_4 inside the capillary of an MWT.

UCl_4 the observed filling is still clearly polycrystalline in nature, with individual crystallites 30–80 Å long abutting onto each other to form continuous but randomly oriented filling. For example, the crystallites denoted **III** (measured as 2.75 Å) and **IV** in Fig. 2b can be seen in different orientations with their (202) and (200) oriented parallel to the

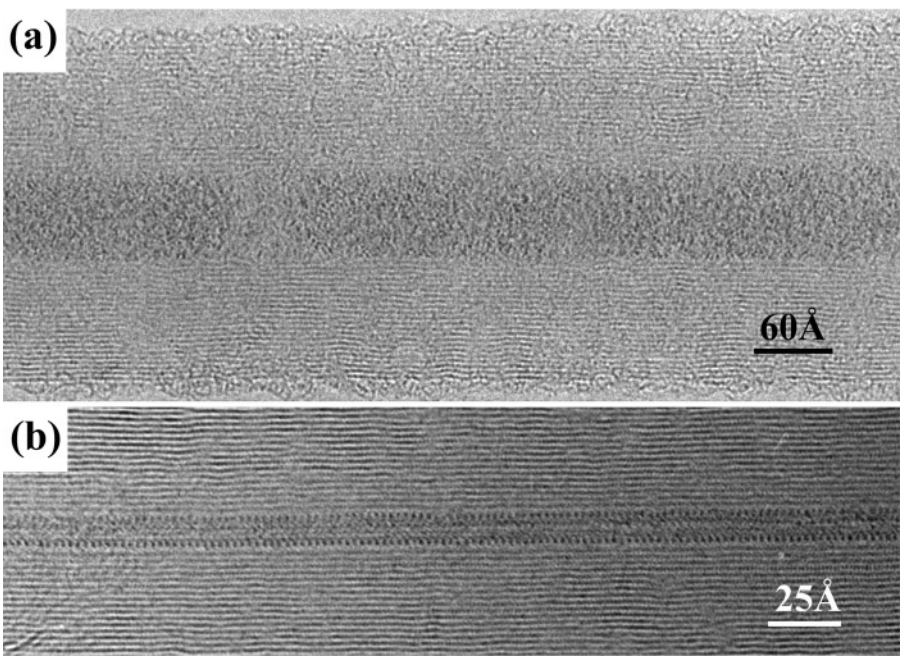

FIG. 3. (a) Micrograph showing amorphous filling obtained when MWTs are filled with 1 : 1 KCl/UCl_4 eutectic mixture (composition B. Fig. 1). (b) Micrograph showing thin capillary MWT filled with composition B. Note continuous, crystalline nature of product.

electron beam. For the crystallite denoted **V**, (202) and (20$\bar{2}$) lattice fringes can be observed at 90° to each other, indicating that this crystallite is viewed in [010] projection. The observed *d*-spacings of all of the observed UCl_4 crystallites are recorded in Table 2b.

Two types of filling were obtained when the 50 mol% KCl : 50 mol% UCl_4 eutectic composition (composition B, Fig. 1) was utilized. The first, illustrated in Fig. 3a, was a continuous amorphous product that filled the entire length of the observed MWT cavities. A second type of continuous filling was also observed in thin capillary MWTs that exhibited a higher degree of crystallinity, as shown by the example in Fig. 3b. EDX analyses indicated that the fillings in both cases contained U, K, and Cl and were consistent with an overall composition of $(KCl)_x(UCl_4)_y$ with x/y ca. 1 : 1. The reason for the partial crystallinity of the filling in Fig. 3b is unclear, but the fact that this effect was observed only in thin capillaries suggests some ordering effect due to the influence of the periodicity of the innermost graphitic layers of the MWTs.

No filling was observed for the composition corresponding to nominal K_2UCl_6 (i.e., composition C, Fig. 1). Instead, large crystals of a single-phase product, presumably corresponding to K_2UCl_6, were observed on the exterior of the MWTs (Fig. 4) only. ED patterns and lattice images indicate that this phase has a distorted hexagonal structure. However, the structure is probably not the same as Na_2UCl_6 (12), which is an ordered $A_xB_yX_{3x}$-type structure and which has a much larger unit cell than indicated by the ED pattern and lattice image, but is possibly a statistical AX_3-type structure (13). A rigorous determination of the crystal structure of this phase was not attempted.

The failure of composition C to fill MWTs is an apparently anomalous result as the composition/surface tension data recorded by Janz *et al.* for the composition 64.31 mol% KCl : 35.69 mol% UCl_4 (see Table 1) seem to indicate that the nearby composition at 66.7 mol% KCl : 33.3 mol% UCl_4 (i.e., K_2UCl_6), ought to fill MWTs easily via capillary action. However, the following points should be made: (i) the surface tension/composition relations of the precise composition range corresponding to K_2UCl_6 was not investigated by Janz *et al.*; (ii) the temperature range investigated (930–1010 K) was above the liquidus of K_2UCl_6 (ca. 900 K). The surface tension properties beneath the liquidus, particularly for single-phase K_2UCl_6, may be radically different (i.e., much higher) than those of the melt.

The filling observed with the second eutectic composition at 73.2% KCl : 26.8% UCl_4 (composition D, Fig. 1) was found to be essentially similar to that observed with the other eutectic composition (composition B, Fig. 1) except that EDX revealed a higher proportion of K in the obtained spectra, consistent with the overall composition $(KCl)_x(UCl_4)_y$ with x/y ca. 2.7 : 1. As with composition B, continuous amorphous filling was observed in large-bore MWTs (Fig. 5a) and continuous crystalline filling was exhibited by narrower bore MWTs (Fig. 5b). Fillings were attempted with compositions to the left of composition D in Fig. 1, but these were found to be mainly amorphous and had a pronounced tendency to melt and disperse after even moderate exposure to the electron beam. For this reason, a proper identification of this material was not possible.

Spiraling Polycrystalline UCl_4 Crystal Growth Observed inside MWTs

In a small number of the MWTs selectively filled with composition A, spirals or zigzags of chains of UCl_4 crystallites could be observed forming the MWT capillaries, as shown by the example in Fig. 6a. In the figure, two spirals of similar length exhibiting an average pitch of ca. 200 Å can

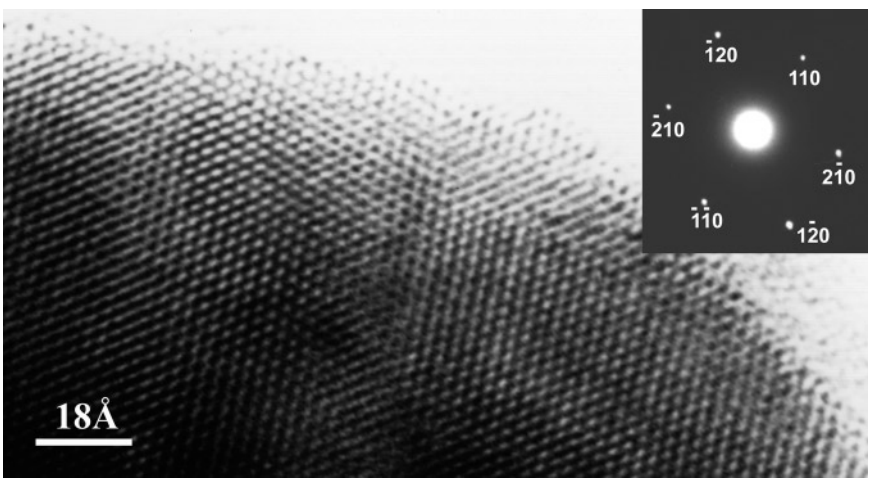

FIG. 4. Micrograph showing dense crystalline product observed formed on the outside of MWTs only corresponding to K_2UCl_4 (composition C, Fig. 1).

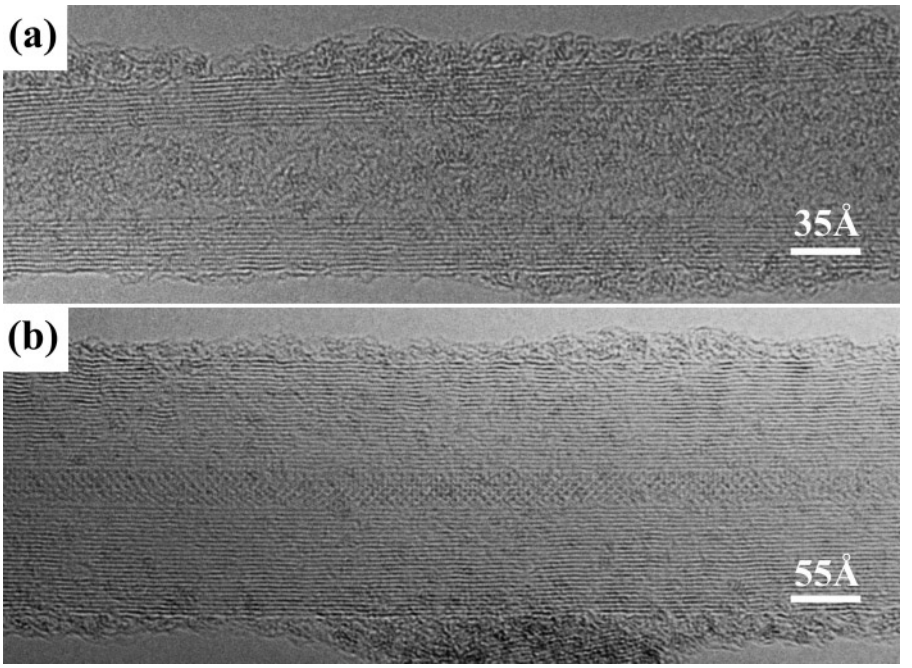

FIG. 5. (a) Micrograph showing continuous amorphous filling obtained when second eutectic composition (composition D) was used to fill MWTs. Note that the filling is lower in contrast than that observed in Fig. 2a because of lower UCl_4 content, (b) Micrograph showing thin capillary MWT filled with composition D. Note that this filling is also continuous and apparently crystalline in nature (cf. Fig. 3b).

be observed. The crystallites within an individual chain are not all simultaneously in focus, which suggests that their arrangement within a chain may be helical rather than two-dimensional. The arrangement is represented schematically in Fig. 6b. We have recently reported a similar phenomenon with respect to spiraling chains of SnO crystallites encapsulated inside MWTs (5). In the case of SnO, the polycrystalline filling was produced by pH-controlled precipitation from aqueous solution rather than by capillarity.

Two explanations can be put forward in order to explain why chains of SnO and UCl_4 crystallites form spirals inside MWTs: (i) the chains of crystals spiral as a result of a van der Waals type interaction between the helically arranged MWT walls (the helical nature of MWTs is one of their fundamental properties (1, 14)) and the crystallite chains; (ii) the crystals spiral as a result of localized compressive force inside the MWT capillary arising during the crystallization process, i.e., as chains of individual crystals nucleate and eventually press against one another, the compression

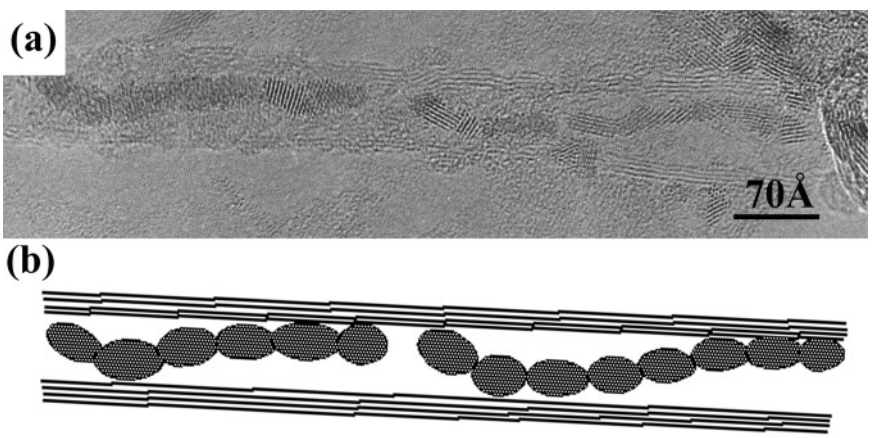

FIG. 6. (a) Micrograph showing spiraling of chains of UCl_4 inside carbon nanotubes. Two spirals with an average pitch of ~ 200 Å can be seen inside the capillary of the nanotube. (b) Schematic representation of (a).

causes buckling in the crystallite chain, resulting in a spiral. This effect can be modeled by observing the packing of hard spheres (e.g. ball bearings) of diameter x cm in a smooth vertical tube of diameter $> 0.5x$ but less than $2x$. Given the relatively weak nature of (i) in comparison to (ii), the latter explanation may be considered to be the most viable.

Oxidation of UCl_4 outside and inside MWTs

HRTEM and EDX examination of the oxidized specimen (originating from composition A) showed that most of the UCl_4 deposited on the outside of the MWTs had oxidized. Figure 7a shows a small quantity of finely divided and partially oxidized UCl_4 situated at the point of contact between two touching MWTs. This material can be seen to be coated by a thin layer of low-contrast amorphous material, which can also be seen both on the outside of the MWT. EDX showed that this material to contain K, U, Cl, and O. Most of the UCl_4 contained within carbon MWTs was found to be unoxidized. Figure 7b shows a MWT filled with polycrystalline UCl_4 which is also coated with amorphous oxidized material similar to that in Fig. 7a. The unoxidized material can be identified from the lattice fringes and the crystallites denoted **VI**, **VII**, **VIII**, and **IX** in Fig. 7b all conform to the (202) plane of UCl_4 (see Table 2b). Note that each crystallite is in a different orientation.

In a small number of MWTs ($\sim 2\%$) a solid continuous filling could be observed corresponding to an oxidized phase of the form $U(Cl, O)_x$ (Fig. 7c). The encapsulated material is almost wholly crystalline except in the region nearest the tip of the MWT where the filling has an amorphous microstructure. The d-spacing of the lattice fringes, measured parallel to the MWT axis, corresponds to 5.12 Å, but due to the wide variety of possible intermediate and fully oxidized products of UCl_4, it was not possible to assign this d-spacing to a particular phase. The formation of only a small amount of oxidized material inside the carbon MWTs (Fig. 7a) compared to that observed to form in the finely divided material deposited on the exterior of the MWTs (Fig. 7c) indicates that MWTs behave as a fairly efficient barrier against oxidation.

Interestingly, the oxidized product forms continuously aligned single crystals along the MWT bores (Fig. 7c) as opposed to the discontinuous chains of individual crystallites observed with the unoxidized UCl_4 product (cf. Fig. 2a, b and 7b) This behavior can be explained in the following terms. As the UCl_4 product reacts with the atmosphere, the oxidized product expands to fill the internal volume of the MWT. In doing so, the expanded crystallites are influenced by the morphological control of the MWT walls and align and expand accordingly.

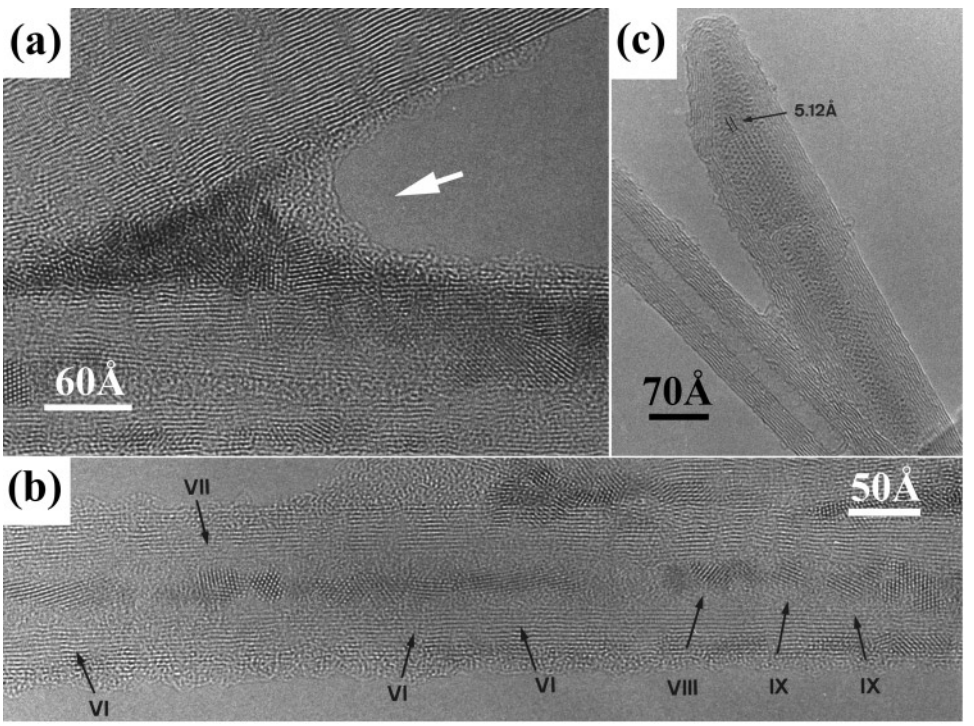

FIG. 7. (a) Micrograph showing finely divided and oxidized material (arrowed) accumulated at the point of contact between two touching nanotubes. (b) Micrograph showing polycrystalline UCl_4 observed in the oxidized specimen. (c) Micrograph showing $U(Cl, O)_x$ filling inside MWT capillary. The d-spacing of the lattice fringes measured parallel to the MWT axis is 5.12 Å.

CONCLUSIONS

This study shows how a simple binary eutectic phase diagram can be used, in conjunction with appropriate surface tension data (15), to establish the correct conditions for selectively filling MWTs and other similar structures (e.g. BN tubes) with various components within a eutectic melting system by capillarity. A UCl_4-enriched noneutectic molten mixture selectively fills MWTs with a polycrystalline, single-phase product. On exposure to the atmosphere, this material slowly oxidizes in air to form $U(Cl, O)_x$. When a low-surface tension eutectic mixture is employed to fill MWTs, continuous filling with amorphous material of the composition $(KCl)_x(UCl_4)_y$ is obtained. Thin capillary MWTs cause these eutectic fillings to partially crystallize resulting in MWTs with continuous crystalline filling.

ACKNOWLEDGMENTS

The authors are indebted to JEOL (Japan) limited for their provision of time on the JEM-2010F microscope and in particular to M. Kawasaki for his assistance with this project. We are also grateful to A. Hobley for repeating some of the preparations.

REFERENCES

1. P. M. Ajayan and S. Iijima, *Nature* **361,** 333 (1993).
2. S. C. Tsang, Y. K. Chen, P. J. F. Harris, and M. L. H. Green, *Nature* **372,** 159 (1994).
3. R. M. Lago, S. C. Tsang, K. L. Lu, Y. K. Chen, and M. L. H. Green, *J. Chem. Soc., Chem. Commun.* **13,** 1355 (1995).
4. P. M. Ajayan, O. Stephan, Ph. Redlich, and C. Coilliex, *Nature* **375,** 564 (1995).
5. J. Sloan, J. Cook, J. R. Heesom, M. L. H. Green, and J. L. Hutchison, *J. Cryst. Growth* **173,** 81 (1997).
6. J. Sloan, J. Cook, M. L. H. Green, J. L. Hutchison, and R. Tenne, *J. Mater. Chem.* **7,** 1089 (1997).
7. Y. K. Chen, M. L. H. Green, and S. C. Tsang, *J. Chem. Soc., Chem. Commun.* 2489 (1996).
8. V. N. Desyatnik and S. P. Raspopin, *Russ. J. Inorg. Chem.* **20,** 780 (1975).
9. G. J. Janz, R. P. T. Tomkins, C. B. Allen, J. R. Downey, Jr., G. L. Gardner, U. Krebs, and S. K. Singer, *J. Phys. Chem. Ref. Data* **4,** 871 (1975).
10. T. W. Ebbesen and P. M. Ajayan, *Nature* **358,** 220 (1992).
11. Powder Diffraction File Card No. 9-56 (ASTM, Philadelphia, PA).
12. P. J. Bendall, A. N. Fitch, and B. E. F. Fender, *J. Appl. Crystallogr.* **16,** 164 (1983).
13. A. F. Wells, *in* "Structural Inorganic Chemistry," 5th ed., p. 447. Clarendon Press, Oxford, 1984.
14. M. Liu and J. M. Cowley, *Carbon* **32,** 393 (1994).
15. For example, see, G. J. Janz, *J. Phys. Chem. Ref. Data* **17,** 109 (1988).